

A NEW SIMPLIFIED CLOSED-FORM INTERACTION FORMULATIONS FOR EVALUATION OF STRUCTURAL RESPONSE OF STIFFENED PLATES

Özgür ÖZGÜÇ*

*Istanbul Technical University, Dept. Of Naval Arch. and Ocean Engineering

ABSTRACT

A semi-analytical model for ultimate strength capacity assessment of stiffened plates has been developed based on ANSYS non-linear elasto-plastic buckling analyses of a wide range of typical ship panel geometries. The primary aim of the present study is to investigate the ultimate strength interaction relationship of a stiffened plate subject to combine loads with imperfections in the form of geometric deflections and welding induced residual stresses. The accuracy of the interaction relationship is confirmed by use of inelastic finite element calculations. Comparison is performed with existing ship rules used by Classification Societies as well. The results and insights derived from the present work are summarized in great detail.

Keywords: Finite Element Analysis; Initial Imperfection; Interaction Formulas; Ship Hull; Ultimate Strength

1. Introduction

Stiffened plates is the main structural building block in ship hulls and their structural response subject to combine loads is a topic of significant practical interest in ship design. Figure 1 shows an example of such construction where the stiffened plate spans between girders. For the real ship structural stiffened plates, the most general loading case is a combination of longitudinal stress, transverse stress, shear stress and lateral pressure. Due to the presence of the combine loads, stiffened panels are susceptible to failure by instability. Instability of stiffened plates can take one of four forms [1,4,5,7] such as plate induced overall buckling (PI), stiffener induced overall buckling (SI), plate buckling (PB) and stiffener tripping (ST). The typical buckling modes are demonstrated in Figure 2.

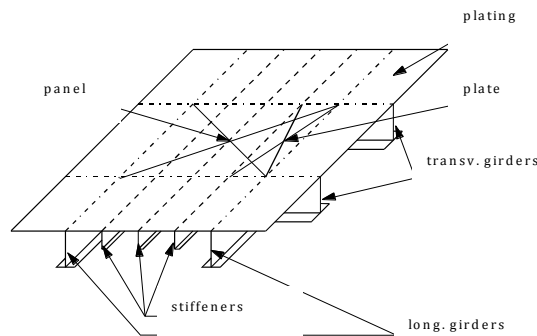


Figure 1. A stiffened steel plate in ship hull

Precise modelling of stiffened panels can be achieved by means of analysis tools and computing power. Initial imperfections such as welding induced residual stress and initial deflections of the cross section can be explicitly incorporated into numerical models. In a series of recent papers,

Grondin [3,4] considered the behaviour of these elements under axial compression, both experimentally and numerically. The goal of that study was to investigate the tripping failure mode and validate with experiments, a sophisticated non-linear finite element model that would allow a more extensive study of the behaviour to be conducted numerically.

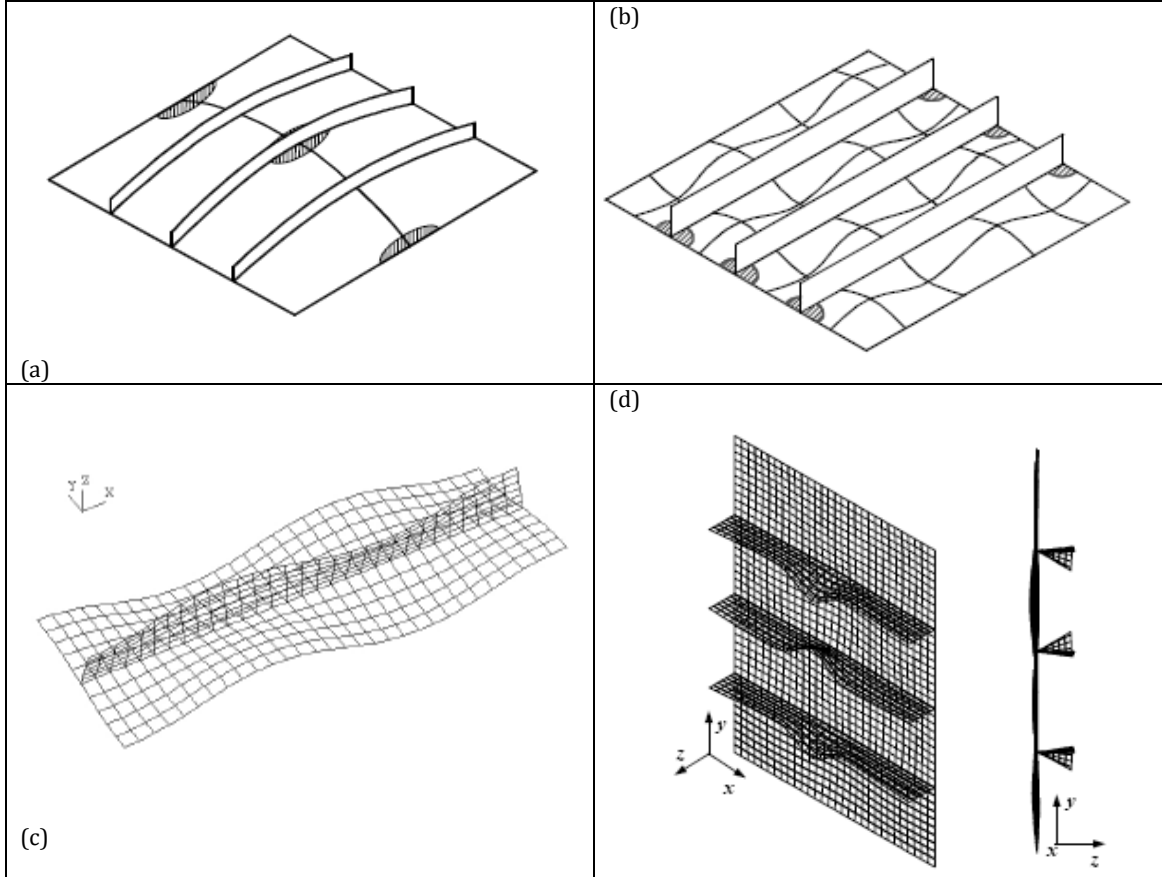


Figure 2. Typical buckling modes, (a) Overall buckling (plate induced); (b) overall buckling (stiffener induced); (c) plate buckling; and (d) stiffener tripping

Hughes, Ghosh and Chen [6] derived modified expressions for elastic local plate buckling and overall panel buckling expressions from 55 Abaqus eigenvalue buckling analyses. Inelastic RISK analysis for the ultimate collapse stress and post collapse behaviour using Abaqus Fem was conducted on their models. Ultimate stress was also calculated using Orthotropic methods. It was found that for panels having crossover proportions, Orthotropic based methods are unsatisfactory. A direct calculation model (PULS) for determination of ultimate capacity of stiffened panels was developed using energy principles and nonlinear plate theory according to Marguerre and Von Karman [9]. Extensive verifications were carried out by means of Abaqus FE program. In general, very satisfactory correspondence between PULS and more advanced numerical programs were found.

Ozguç Et al. [13] developed the new simple design equations for predicting the ultimate compressive strength of stiffened plates with initial imperfections in the form of welding-induced residual stresses and geometric deflections were developed in this study. A non-linear finite element method was used to investigate on 60 ANSYS elastic-plastic buckling analyses

of a wide range of typical ship panel geometries. Reduction factors of the ultimate strength are produced from the results of 60 ANSYS inelastic finite element analyses. The accuracy of the proposed equations was validated by the experimental results. Comparisons show that the adopted method has sufficient accuracy for practical applications in ship design.

Paik Et al. [14] concentrated on methods for the ultimate limit state assessment of stiffened plate structures under combined biaxial compression and lateral pressure actions considering the bottom part of an AFRAMAX-class hypothetical double-hull oil tanker structure. Three methods, namely ANSYS nonlinear finite element method, DNV PULS method, and ALPS/ULSAP method were used.

Chaithanya Et al.. [11] evaluated the behavior of stiffened plates with different distortion levels in order to address a rational structural design procedure, as pre-existing and fabrication-related initial geometrical distortion from a structural design point of view. Non-linear finite element (FE) analysis using ABAQUS was carried out under axial loading condition to predict the behavior and the buckling strength.

Xu and Soares [12] simulated numerically the behavior of stiffened panels under uniaxial compression until collapse and beyond, and then compared with tests made to investigate the influence of the stiffener's geometry and the boundary conditions. The stiffened panel models have three longitudinal bays to produce reasonable boundary conditions in the longitudinal direction. The material and geometric nonlinearities were accounted for in the FE analyses. The initial geometric imperfections, which affect significantly the collapse behavior of stiffened panels, were assumed to have the shape of the linear buckling mode. Four types of stiffeners were made of mild or high tensile steel for bar stiffeners and mild steel for 'L' and 'U' stiffeners to investigate different material and geometry configurations, and four boundary conditions were analyzed.

Tekgoz Et al. [15] analyzed the effect of different finite element models on the ultimate strength assessment of stiffened plates, where the effect of element size, and type, boundary conditions, shape of initial imperfection, thickness and net sectional configurations were accounted for. Four different finite element models and different structural configurations were compared to the solution described by the Common Structural Rules (CSR).

Cho Et al. [16] proposed ultimate strength formulation for stiffened plates. The formulation was derived by a regression study using the parametric study results. The accuracy and reliability of the proposed formulation were compared with those of commercial packages, such as ABAQUS and DNV PULS, and experimental results.

Zhang [17] presented a review and study on ultimate strength analysis methods for steel plates and stiffened panels in axial compression. Buckling and collapsing mechanisms of steel plates and stiffened panels are described. A study and further validation on the authors developed formula for ultimate strength of stiffened panels using a comprehensive non-linear finite element analysis, 110 models in total, and a wide range of model test results, 70 models in total, were carried out. Finally, applications of the developed formula to existing oil tankers and bulk carriers were presented.

The primary aim of the present study is to investigate the ultimate strength interaction relationship of a stiffened plate subject to combine loads with imperfections in the form of

geometric deflections and welding-induced residual stresses. The accuracy of the interaction relationship is confirmed by use of inelastic finite element calculations. Comparison is performed with existing ship rules used by Classification Societies as well. The results and insights derived from the present work are summarized.

2. Simplified Closed-Form Formulations for Collapse Strength

A semi-analytical model for calculating the values of the critical buckling stresses for the plate, beam-column, torsional-flexural (tripping) and local failure modes are developed with reduction factors which can describes initial imperfections in the form of geometric deflections and welding-induced residual stresses. Based on extensive numerical calculations an interaction formula is proposed for combine loading which involves longitudinal compression, transverse compression, shear loading and lateral pressure loading [8].

2.1 Elasto-plastic Collapse of the Structural Elements

The equation describing the load-end shortening curve $\sigma - \varepsilon$ or the elastic-plastic collapse of structural elements composing the hull girder transverse section can be obtained from the following formula, valid for both positive (shortening) and negative (lengthening) strains.

$$\sigma = \Phi \sigma_o \quad (1)$$

where, Φ is edge function, σ_o is yield stress of element.

$$\Phi = \begin{cases} -1 & \text{for } \varepsilon < -1 \\ \varepsilon & \text{for } -1 < \varepsilon < 1 \\ 1 & \text{for } \varepsilon > 1 \end{cases} \quad (2)$$

2.2 Beam – column Buckling Failure Model

The equation describing the load-end shortening curve $\sigma_{CR1} - \varepsilon$ for the beam-column buckling of the stiffeners composing the hull girder transverse section can be obtained from the following formula:

$$\sigma_{CR1} = \Phi \sigma_{C1} \left(\frac{A_S + b E t}{A_S + b t} \right) \quad (3)$$

where, Φ is edge function defined in equation 1, σ_{C1} is critical stress in MPa, A_S is net

sectional area of a stiffener and b is spacing of stiffeners.

$$\sigma_{C1} = \begin{cases} \frac{\sigma_{E1}}{\varepsilon} & \text{for } \sigma_{E1} \leq \frac{\sigma_o}{2} \varepsilon \\ \sigma_o \left(1 - \frac{\Phi \sigma_o \varepsilon}{4 \sigma_{E1}} \right) & \text{for } \sigma_{E1} > \frac{\sigma_o}{2} \varepsilon \end{cases} \quad (4)$$

where σ_{C1} is based on the Johnson-Ostenfeld formulation accounting for inelastic effects on the column's buckling. In equation (3) the second term computes the loss of efficiency of plate due to compression loading. Effective width, b_E , based on the Frankland's approach developed to the plate strength and given by,

$$b_E = \begin{cases} b & \text{for } \beta_E \leq 1.25 \\ \left(\frac{2.25}{\beta_E} - \frac{1.25}{\beta_E^2} \right) b & \text{for } 1.25 < \beta_E \leq 3.25 \\ \left(\frac{1.91}{\beta_E} \right) b & \text{for } \beta_E > 3.25 \end{cases} \quad (5)$$

where, σ_{E1} is Euler column buckling stress, which is calculated as below,

$$\sigma_{E1} = \pi^2 E \frac{I_E}{A_E a^2} \quad (6)$$

where, I_E is net moment of inertia of ordinary stiffeners with attached shell plating of width b_{E1} , A_E is net sectional area of stiffeners with attached shell plating of effective width b_E , and a is length of stiffened plate.

$$b_{E1} = \begin{cases} \frac{b}{\beta_E} & \text{for } \beta_E > 1 \\ b & \text{for } \beta_E \leq 1 \end{cases} \quad (7)$$

where, $\beta_E = \frac{b}{t} \sqrt{\frac{\varepsilon \sigma_o}{E}}$ is defined.

2.3 Plate induced buckling failure mode

The equation describing the load-end shortening curve $\sigma_{CR2} - \varepsilon$ for the plate buckling composing the hull girder transverse section can be obtained the following formula:

$$\sigma_{CR2} = \Phi \left(\frac{A_S + b_E t}{A_S + bt} \right) \quad (8)$$

2.4 Flexural – torsional (tripping) Buckling Failure Mode

The equation describing the load-end shortening curve $\sigma_{CR3} - \varepsilon$ for the flexural – torsional (tripping) buckling of stiffeners composing the hull girder transverse can be obtained according to following formula:

$$\sigma_{CR3} = \Phi \left(\frac{A_S \sigma_{C3} + bt \sigma_{CP}}{A_S + bt} \right) \quad (9)$$

where, σ_{C3} is defined as critical stress.

$$\sigma_{C3} = \begin{cases} \frac{\sigma_{E3}}{\varepsilon} & \text{for } \sigma_{E3} \leq \frac{\sigma_o}{2} \varepsilon \\ \sigma_o \left(1 - \frac{\Phi \sigma_o \varepsilon}{4 \sigma_{E3}} \right) & \text{for } \sigma_{E3} > \frac{\sigma_o}{2} \varepsilon \end{cases} \quad (10)$$

where, σ_{E3} is Euler torsional buckling stress, defined as follows.

$$\sigma_{E3} = \frac{\pi^2 EI_W}{I_P a^2} \left(\frac{K_C}{m^2} + m^2 \right) + 0.385 E \left(\frac{I_t}{I_P} \right) \quad (11)$$

where, I_w is net sectional moment of inertia of the stiffener about its connection to the attached plating and is defined as follows.

$$I_w = \begin{cases} \frac{h_w^3 t_w^3}{36} & \text{for flat bars} \\ \frac{t_f b_f^3 h_w^2}{12} & \text{for T-sections} \\ \frac{b_f^3 h_w^2}{12 (b_f + h_w)^2} [t_f b_f^2 + 2b_f h_w + 4h_w^2 + 3t_w b_f h_w] & \text{for angles and bulb sections} \end{cases} \quad (12)$$

where, I_P is net polar moment of inertia of the stiffener about its connection to the attached plating, defined as follows.

$$I_P = \begin{cases} \frac{h_w^3 t_w}{3} & \text{for flat bars} \\ \left(\frac{h_w^3 t_w}{3} + h_w^2 b_f t_f \right) & \text{for stiffeners with face plate} \end{cases} \quad (13)$$

where, I_t is St. Venant's net moment of inertia of stiffener without attached plating, defined as follows:

$$I_t = \begin{cases} \frac{h_w t_w^3}{3} & \text{for flat bars} \\ \frac{1}{3} \left[h_w t_w^3 + b_f t_f^3 \left(1 - 0.63 \frac{t_f}{b_f} \right) \right] & \text{for stiffeners with face plate} \end{cases} \quad (14)$$

where, m is number of half waves, may be taken equal to the integer number and K_c is torsional buckling of axially loaded stiffeners, calculated by following;

$$m^2(m-1)^2 \leq K_c < m^2(m+1)^2 \quad \text{and} \quad K_c = \left(\frac{C_0 a^4}{\pi^4 EI_w} \right) \quad (15)$$

where, C_0 is a spring stiffener of the attached plating and can be expressed as follows,

$$C_0 = \frac{Et^3}{2.73b} \quad (16)$$

Table 1. Torsional buckling of axially loaded stiffeners – Number of m half waves.

K_c	$0 \leq K_c < 4$	$4 \leq K_c < 36$	$36 \leq K_c < 144$
m	1	2	3

where, σ_{cp} is buckling stress of attached plating, which can be determined by following formula.

$$\sigma_{cp} = \begin{cases} \sigma_o & \text{for } \beta_E \leq 1.25 \\ \left(\frac{2.25}{\beta_E} - \frac{1.25}{\beta_E^2} \right) \sigma_o & \text{for } 1.25 < \beta_E \leq 3.25 \\ \left(\frac{1.91}{\beta_E} \right) \sigma_o & \text{for } \beta_E > 3.25 \end{cases} \quad (17)$$

2.5 Web Local Buckling Failure Mode

The equation describing the load-end shortening curve $\sigma_{CR4} - \epsilon$ for the web local buckling of flanged stiffeners composing the hull girder transverse section can be obtained from the following formula.

$$\sigma_{CR4} = \Phi \sigma_o \left(\frac{b_E t + h_{we} t_w + b_f t_f}{bt + h_w t_w + b_f t_f} \right) \quad (18)$$

where, h_{we} is effective height of the web, which can be determined by following formula:

$$h_{we} = \begin{cases} h_w & \text{for } \beta_w \leq 1.25 \\ \left(\frac{2.25}{\beta_E} - \frac{1.25}{\beta_E^2} \right) h_w & \text{for } 1.25 < \beta_w \leq 3.25 \\ \left(\frac{1.91}{\beta_E} \right) h_w & \text{for } \beta_w > 3.25 \end{cases} \quad (19)$$

$\beta_w = \frac{h_w}{t_w} \sqrt{\frac{\varepsilon \sigma_o}{E}}$ is defined while ε is relative strain.

Effective width, b_E is multiplied by reduction factors so as to introduce initial imperfections for stiffened plates, namely,

$$b_E^i = b_E R_d R_r R_y R_\tau R_q \quad (20)$$

where b_E^i is the effective width of imperfect stiffened plate, b_E is the effective width of perfect stiffened plate, R_d is a reduction factor due to initial deflection, R_r is a reduction factor due to welding-induced residual stress, R_y is a reduction factor due to bi-axial compression, R_τ is a reduction factor due to shear stress present, and R_q is a reduction factor due to lateral pressure load. All reduction factors proposed are expressed by the following equations:

$$R_d = 1.0 - 0.2323 f(\lambda)g(\beta) \quad (21)$$

$$f(\lambda) = \begin{cases} 0.015 & \text{for } 0 < \lambda \leq 0.35 \\ (-1.03 + 2.341 \lambda - 1.344 \lambda^2 + 0.212 \lambda^3) & \text{for } \lambda > 0.35 \end{cases} \quad (22)$$

$$g(\beta) = \begin{cases} (10.818 + 0.204\beta - 5.177\beta^2) & \text{for } 1 < \beta \leq 1.5 \\ (4.594 - 0.805\beta + 0.255\beta^2) & \text{for } 1.5 < \beta \leq 2.0 \\ (6.404 - 1.847\beta + 0.371\beta^2) & \text{for } 2 < \beta \leq 2.5 \\ (5.435 - 1.213\beta + 0.202\beta^2) & \text{for } 2.5 < \beta \leq 4.0 \end{cases} \quad (23)$$

$$R_r = 1.0 - \left[\frac{\mu}{8.1(\beta - 1.901)^2 + 1} \right] \quad (24)$$

where $\mu = \left(\frac{\sigma_r}{\sigma_o} \right)$ is defined as normalized welding residual stress.

$$R_y = 1.0 - \left(\frac{\sigma_y}{\sigma_{yu}} \right)^2 \quad (25)$$

which is proposed by Faulkner [2], where $\sigma_y \leq 0.25 \sigma_o$

$$\sigma_{yu} = \sigma_o \left(\frac{0.9}{\beta^2} + \frac{1.9}{\alpha\beta} \left(1 - \frac{0.9}{\beta^2} \right) \right) \quad (26)$$

$$R_q = (1.0 + 0.0262 \xi - 0.3232 \xi^2) \quad (27)$$

where $\xi = \left(\frac{\rho E}{\sigma_o^2} \right)$ is defined as normalized value of pressure.

$$R_\tau = \left[1 - \left(\frac{\tau}{\tau_o} \right)^2 \right]^{0.5} \quad (28)$$

where $\tau_o = \frac{\sigma_o}{\sqrt{3}}$ is given by Faulkner [2].

Initial deflection value is taken into account for plating and stiffeners implicitly in this study.

For clamped stiffened plates, b_E , effective width may be re-arranged by the following simple equations as well.

$$b_E = \begin{cases} 1.035 b & \text{for } \beta_E \leq 1.25 \\ \left(\frac{2.65}{\beta_E} - \frac{1.95}{\beta_E^2} \right) b & \text{for } 1.25 < \beta_E \leq 3.25 \\ \left(\frac{1.95}{\beta_E} \right) b & \text{for } \beta_E > 3.25 \end{cases} \quad (29)$$

where β is the slenderness ratio, λ is beam-column slenderness ratio, $\left(\frac{\sigma_r}{\sigma_o} \right)$ is normalized compressive welding-induced stress, $\left(\frac{w_o}{t} \right)$ is non-dimensional initial deflection, τ is shear stress, σ_y is transverse stress and p is lateral pressure load.

Ship plates in decks and bottoms are predominantly loaded in longitudinal compression. However, additional loading systems may result in the simultaneous presence of transverse in plane and shear loads in addition to lateral loading of the plates. The influences of these loads on the collapse strength of plates can be very significant. Based on extensive numerical results an interaction curve is suggested for practical applications in ship design.

$$\left(\frac{\sigma_x}{\sigma_{xu}} \right)^2 + \left(\frac{\sigma_y}{\sigma_{yu}} \right)^2 + \left(\frac{\tau}{\tau_u} \right)^{3.5} + \left(\frac{p}{p_u} \right)^{1.5} = 1 \quad (31)$$

where p_u is defined as critical (ultimate) lateral pressure of plating between stiffeners clamped at all edges from rigid plastic theory proposed by Wood [10] as below:

$$p_u = C_p \frac{\sigma_{op}^2}{E \beta^2}, \text{ where } C_p = \frac{12}{\left[\sqrt{3 + (b/a)^2} - b/a \right]^2} \quad (32)$$

3. Finite Element Model for Inelastic Buckling Analyses

Authors investigated the structural ultimate capacity of the geometrical properties of the 60 three-bay panels having three and five equally spaced T-stiffeners under combine loads using ANSYS Implicit non-linear finite element code [8]. All models were 3600 mm wide and it was intended that they cover the full range of proportions of typical ship plates. A few models are addressed in this paper. An elastic perfectly plastic material model without strain hardening may be considered enough for pessimistic strength assessment of stiffened steel plates. Arc-length method is applied to the solving of non-linear finite element stiffness equations. The material yielding stress, σ_o , is 352.8 MPa, Young's modulus, E , 205800 MPa and the poisson ratio, ν , is assumed to be 0.30. Four-nodded shell elements are used to model stiffened plate, and a fine mesh is conducted to adequately capture the stress and deformations. One of the examples of all investigated models is shown in Figure 3.

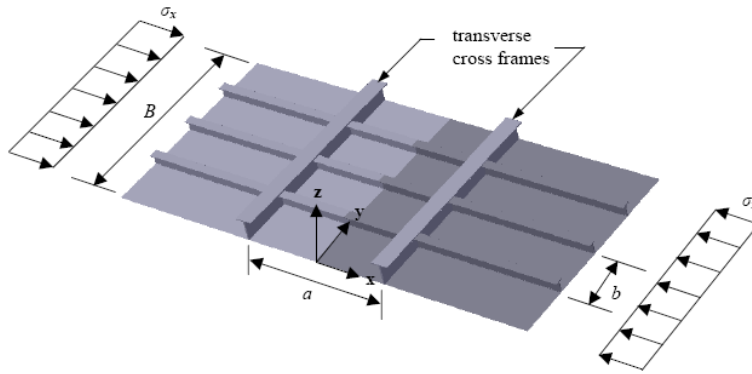
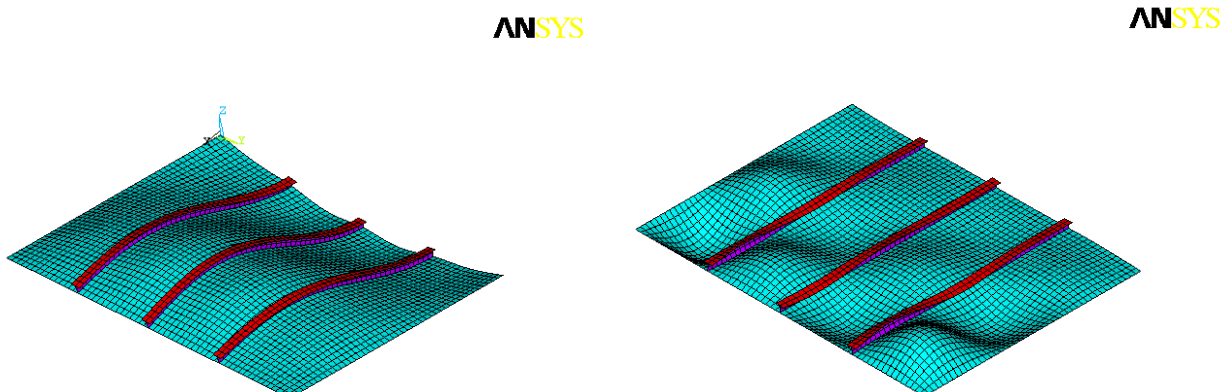


Figure 3. ANSYS solid model for three-bay grillages in this study

3.1 Initial Imperfections for ANSYS FE Model

It is assumed that plating has the overall buckling mode initial deflection, which corresponds to $0.05 \beta^2 t$. The column-type or sideways initial deflection of the stiffeners is taken into account to be $0.0025 a$, where a is the length of one-bay. Initial deflection of plating and stiffeners is automatically accounted once the scaling factor is applied which corresponds to above assumed equations. The imperfection patterns are determined from an overall buckling mode shape of a linear eigenvalue buckling analysis. The considered mode shape has an upward half wave deflection in the full bay and a downward deflection in the half bay, which is shown with the local plate-buckling mode of a three-stiffener panel in “Figure 4”.

Figure 4. Overall buckling and local plate-buckling mode shapes of a three-stiffener panel, respectively



For residual stress distribution Faulkner’s model is used to represent the distribution of the stresses, and is incorporated into ANSYS finite element model as a simple representation of the actual residual stress present in the stiffened panels. The tensile regions around the stiffeners represented as a tension block having base width proportional to the plate thickness ($\eta \times t_{plate}$) where the value of η typically ranges 3.5 and 4 in a ship structures. It is considered to be 3.5 in this study.

3.2 Comparison between ANSYS FEM and Simplified Closed-form Formulations

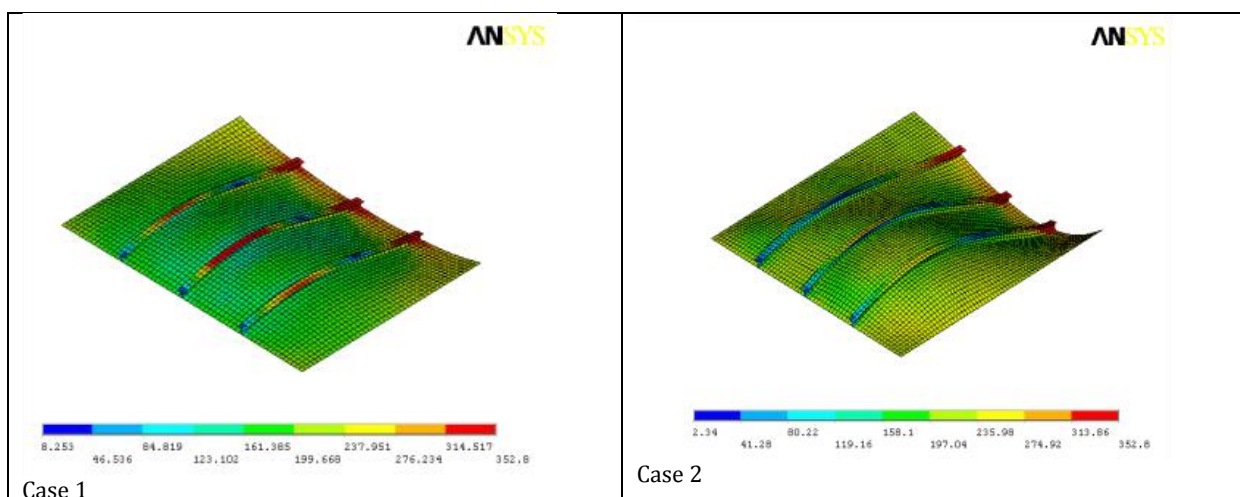
From extensive FE non-linear numerical calculations, four cases are addressed in this paper. Typical ship panel geometries studied are summarized in Table 2.

Table 2. Geometric properties of stiffened panels analyzed in this paper

Specimen no.	β (Plate Slenderness)	λ (Beam-column slenderness)	α (Aspect ratio)	Plate initial deflection (mm) ($0.05\beta^2t$)	Stiffener initial deflection (mm) ($0.0025a$)	Residual Stress for stiffened plate (MPa)	σ_{op} (MPa)	σ_{ow} (MPa)	σ_{of} (MPa)
Case 1	1.77	0.83	2.00	3.30	4.50	35.3	352.8	352.8	352.8
Case 2	1.77	0.86	2.94	3.30	6.60	35.3	352.8	352.8	352.8
Case 3	1.55	0.72	4.40	1.93	6.60	35.3	352.8	352.8	352.8
Case 4	2.48	1.22	4.40	3.08	6.60	35.3	352.8	352.8	352.8

3.3 Computed FE Results

Figure 4 indicates Von Mises stress distributions obtained from ANSYS, while Figure 5 shows stress-strain relationships with considering initial deflection effects from simple design equations and ANSYS FEM as well.



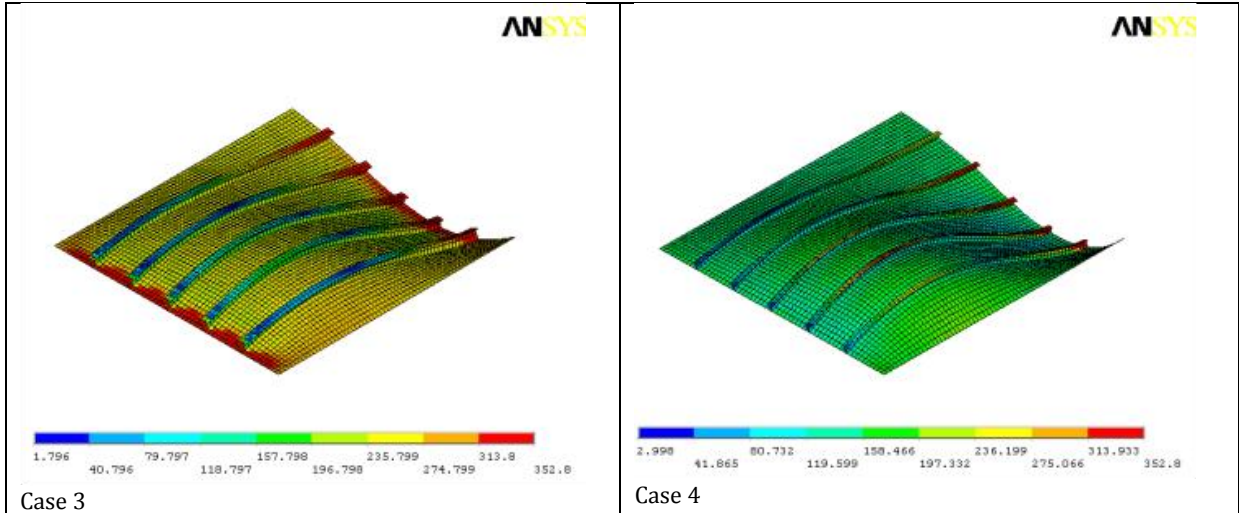


Figure 4. Von Mises stress distribution with ignoring residual stress for considered all cases, Case1, Case2, Case3 and Case 4, respectively

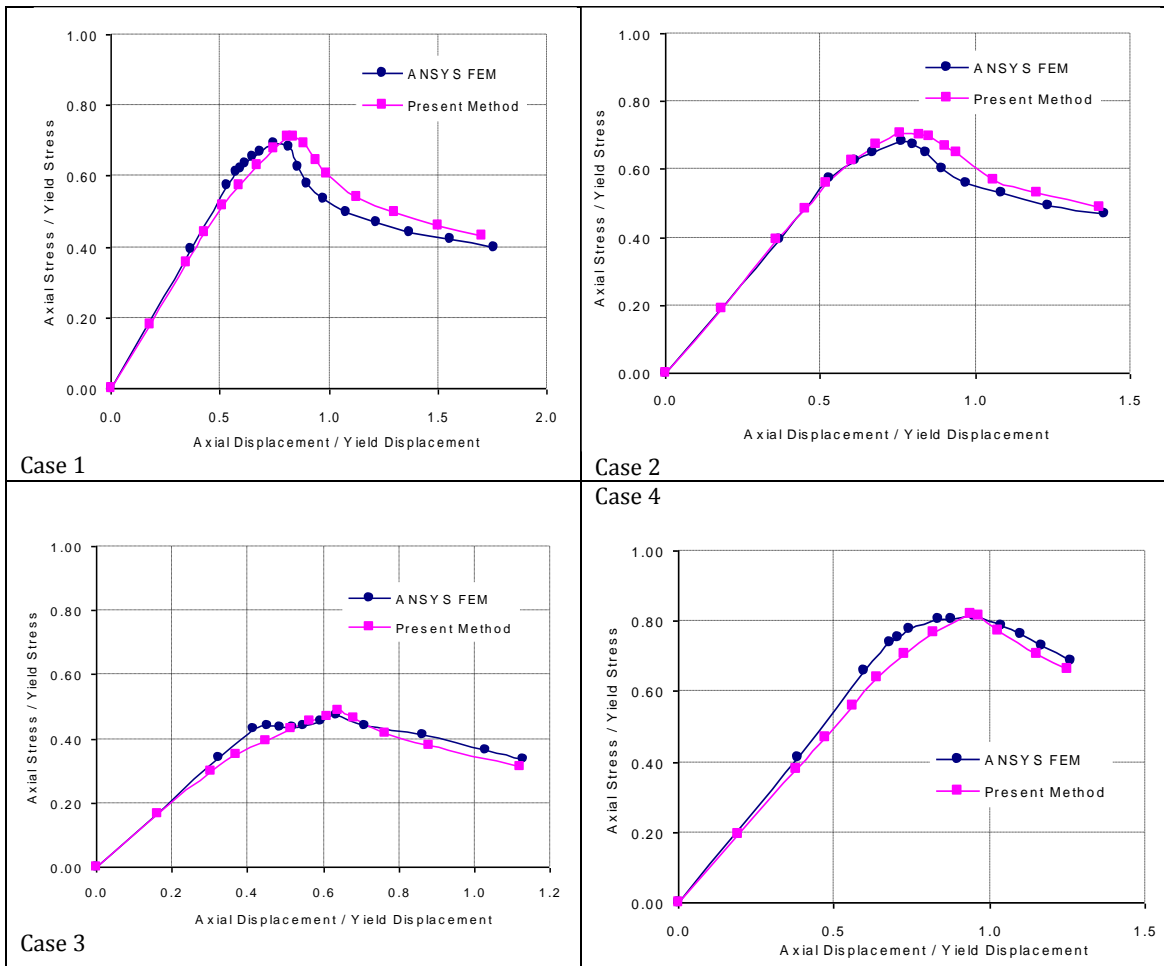


Figure 5. Comparison of ANSYS FEM with approximate formulation for Case1, Case2, Case3 and Case 4, respectively with initial deflection effect

As demonstrated, collapse behaviour of structural members composing a cross section of a hull girder largely affects the collapse behaviour of the cross section and its ultimate strength as whole. From this viewpoint, it is very important to know how accurately the applied method simulates the collapse response and predicts the ultimate strength of individual structural members as stiffened plates. Comparisons of ultimate strength capacities using ANSYS FEM and simplified closed-form formulations are very consistent for all cases studied in this paper.

3.4 Interaction Capacity Curve

New proposed interaction formula is also validated results reported by DNV Research Team [6]. In this paper, capacity curves for combined loads calculated by ABAQUS, DNV PULS, DNV and GL rules are presented with present method.

3.5 Biaxial Compression

Capacity curves for bi-axial compression of bottom panel of a 173 m tanker are presented in Figure 6, while Table 3. summarizes main particulars of investigated model. Results for the same panel under combined in-plane compression and lateral pressure are presented in Figure 7.

Table 3. The main particulars of the tanker bottom panel.

Length of stiffened panel	2400 mm
Stiffener spacing	800 mm
Plate thickness	13.5 mm
Web height	240 mm
Web thickness	11 mm
Stiffeners	6 longitudinal Bulb profiles
Yield stress	355 MPa
Young's modulus	208000 MPa
Poisson ratio	0.3

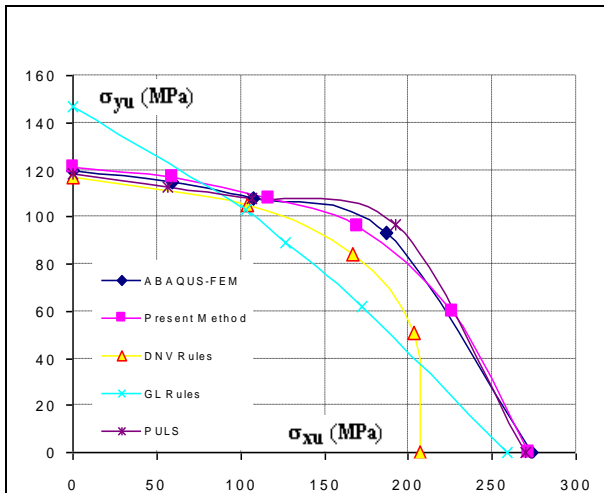


Figure 6. Tanker bottom panel, biaxial compression without lateral pressure

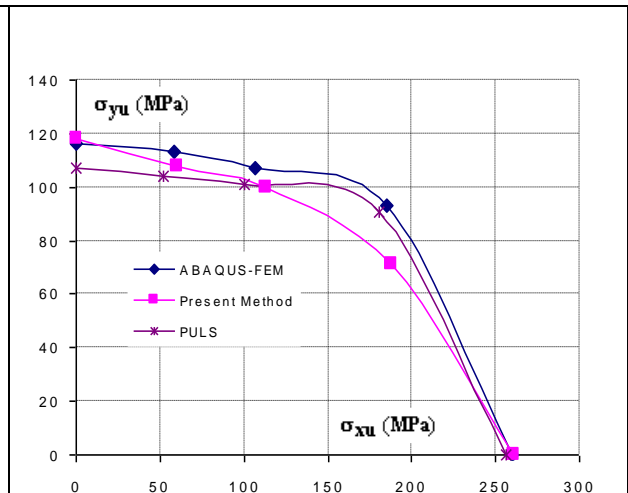


Figure 7. Tanker bottom panel, biaxial compression with lateral pressure, $p = 0.151$ MPa

The comparisons of ultimate strength capacities using ABAQUS, PULS and present method are very consistent. Such deviations are to be expected since the applied methods are very different. Typically, the largest deviations are for regions in load space where the failure mode is not unique and obtained results depend strongly on how the geometrical imperfections are modelled

especially with respect to shape and definition of boundary condition. It is seen that reduction in the in-plane capacity is not very much reduced when the design lateral pressure is employed. The reduction is somewhat lesser for present method than ABAQUS and PULS.

It is seen that present approach predicts more capacity than both of the rule formulations in the bi-axial region. For pure axial compression, DNV Rules seem to be overly conservative when compared with all prediction methods, while for pure transverse compression GL Rules seem to be non-conservative. The present method curve is more convex, which is also the case for ABAQUS, PULS and DNV Rules, while the GL Rules interaction curve is close to linear.

3.6 Effect of Shear Load

Capacity curves for combined shear load and transverse compression of a bulk carrier side panel are presented in Figure 8, while Table 4. summarizes main particulars of investigated model. The loading is typically compression perpendicular to the stiffener transverse direction acting simultaneously with in-plane shear and lateral pressure from the sea. Results for the same panel under combined transverse compression, shear and lateral pressure are presented in Figure 9.

Table 4. The main particulars of the Bulk Carrier side panel.

Length of stiffened panel	8800 mm
Stiffener spacing	890 mm
Plate thickness	14.5 mm
Web height	700 mm
Web thickness	13 mm
Stiffeners	5 longitudinal Tee profiles
Flange breadth	150 mm
Flange thickness	18 mm
Yield stress	355 MPa
Young's modulus	208000 MPa
Poisson ratio	0.3

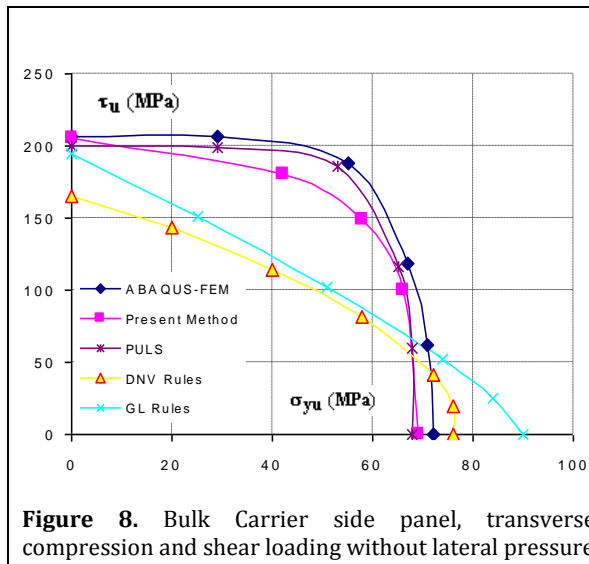


Figure 8. Bulk Carrier side panel, transverse compression and shear loading without lateral pressure

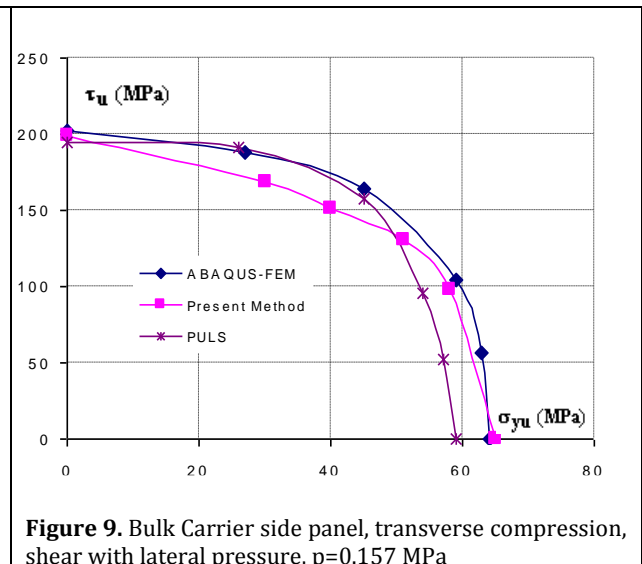


Figure 9. Bulk Carrier side panel, transverse compression, shear with lateral pressure, $p=0.157$ MPa

It can be seen that present method shows very reasonable results as compared to ABAQUS and PULS analyses covering load combinations covering load combinations dominated by shear

loading as well as load combinations dominated by transverse compression. The presence of lateral pressure is not very significant for the in-plane capacity of this pane, though more so for transverse dominated loading than for pure shear. It is seen that both the rule formulations overpredict the capacity for pure transverse compression, while they significantly underestimate the capacity in the combined load region of the capacity curve.

3.7 Effect of Lateral Pressure

Capacity curves for the axial capacity for a tanker bottom panel are presented as a function of lateral pressure in Figure 10, while Table 5. summarizes main particulars of investigated model. The transverse capacity for the same panel is presented as a function of lateral pressure in Figure 11.

Table 5. The main particulars of the tanker bottom panel.

Length of each bay (mm)	5120
Panel breadth (mm)	9100
Plate thickness (mm)	20
Web height (mm)	598.5
Web thickness (mm)	12
Stiffeners	9 longitudinal T-stiffeners
Flange breadth (mm)	200
Flange thickness (mm)	20
Yield stress (MPa)	315
Young's modulus (MPa)	208000
Poisson ratio	0.30

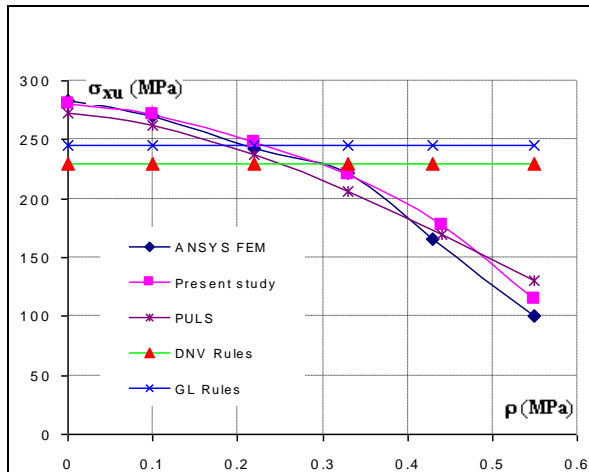


Figure 10. Effect of lateral pressure on axial capacity for tanker bottom panel

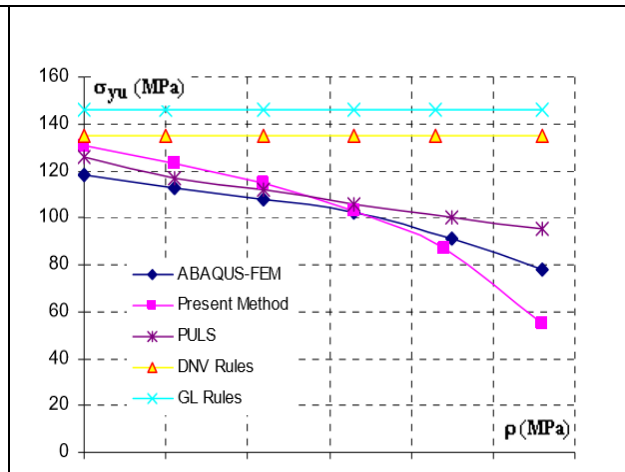


Figure 11. Effect of lateral pressure on transverse capacity for tanker bottom panel

It is seen that present method in the axial capacity predicts reasonable results as compared to ABAQUS, while the rule formulations overpredict the capacity of the panel since they are not affected by influence of lateral pressure.

It is seen that present method in the transverse capacity estimate slightly more results up to 0.20 MPa since transverse capacity overpredicts when lateral pressure is zero, however, it estimates very good at 0.30 MPa, where it underestimates at fixed pressure of 0.55 MPa. Rule formulations overpredict transverse capacity even for zero lateral pressure and more so for increasing magnitude of pressure. The results indicate that lateral pressure has important influence on the buckling capacity and should be taken into account.

4. Discussion and Conclusion

Simplified closed-form interaction formulations for the ultimate capacity assessment of stiffened panels has been developed based on a large number of non-linear finite element analyses using the commercial program ANSYS. It is believed that full nonlinear finite element codes are able to predict buckling deflection an accuracy which is sufficient for advanced design purposes, on condition that the analyses are done properly such as boundary conditions, mesh size, model extent, element types and imperfections. Validation of the proposed model is conducted by use of non-linear finite element calculations and by existing ship rules used by DNV and GL Rules. It is found that present model is generally consistent with results obtained from by ABAQUS and PULS. The rules used by Classification Societies are found to be conservative for some case and non-conservative for other cases as compared with ABAQUS and PULS. Therefore, it is difficult to assess the actual safety margin using these formulations. The main advantage of the approximate method relative to FEM results from the time consumption both in the creation of model and in the CPU time, so it can be used for practical applications in ship design.

References

- [1] Bonello, M.A.; Chryssanthopoulos, M.K.; Dowling, P.J. Ultimate Strength Design of Stiffened Plates under Axial Compression and Bending, *Marine Structure*, 1993, Vol. 6, pp. 532-552.
- [2] Faulkner, D. A review of Effective Plating for use in the Analysis of Stiffened Plating in Bending and Compression, *Journal of Ship Research*, 1975, Vol. 19, No. 1, pp. 1-17.
- [3] Grondin, G.Y.; Chen, Q.; Elwi A.E.; Cheng J.J.R. Buckling of Stiffened Steel Plates- Validation of a Numerical Model, *Journal of Constructional Steel Research*, 1998, Vol. 45, No. 2, pp. 125-148.
- [4] Grondin, G.Y.; Chen, Q.; Elwi, A.E.; Cheng J.J.R. Buckling of Stiffened Steel Plates- A Parametric Study, *Journal of Constructional Steel Research*, 1999, Vol. 50, No. 2, pp. 151-175.
- [5] Hu, S.Z.; Chen, Q.; Pegg, N.; Zimmercman, T.J.E. Ultimate Collapse tests of Stiffened Plate Ship Structural Units, *Marine Structure*, 1997, Vol. 10, pp. 587-610.
- [6] Hughes, O.F.; Ghosh, B.; Chen, Y. Improved Prediction of Simultaneous Local and Overall Buckling of Stiffened Panels, *Thin-Walled Structures*, Vol. 42, pp. 827-856, 2004. [7] Murray N.W., Buckling of Stiffened Panel Loaded Axially and in Bending. *Structure Engineer*, 1973, Vol. 51, No. 8, pp. 285-301.
- [7] Steen, E.; Byklum, E.; Vilming, K.; Ostvolds, K. Computerized Buckling Models for Ultimate Strength Assessment of Stiffened Ship Hull Panels, 9th Symposium on Practical Design of Ships and Other Floating Structures, 2004, Luebeck-Travemuende, Germany.
- [8] Wood, R.H. Plastic and Inelastic Design of Slabs and Plates, The Ronald Press, 1961, New York.
- [9] Chaithanya, P.P.; Das, P.K.; Crow, A.; Hunt, S. The effect of distortion on the buckling strength of stiffened panels. *Ships and Offshore Structures*, 2010, Vol.5.

- [10] Xu, M.C.; Soares, C.G. Numerical assessment of experiments on the ultimate strength of stiffened panels, *Engineering Structures*, 2012, Vol.45, pp. 460–471.
- [11] Ozguc, O.; Das, P.K.; Barltrop, N. The new simple design equations for the ultimate compressive strength of imperfect stiffened plates. *Ocean Engineering*, 2007, Vol. 34, Issue 7, pp. 970–986.
- [12] Paik, J.K.; Kim, B.J.; Seo, J.K. Methods for ultimate limit state assessment of ships and ship-shaped offshore structures: Part II stiffened panels. *Ocean Engineering*, 2008, Volume 35, Issue 2, pp. 271–280.
- [13] Tekgoz, M.; Garbatov, Y.; Soares, C.G. Ultimate strength assessment for the effect of finite element modelling. *Maritime Engineering and Technology*, 2012.
- [14] Cho, S.R.; Kim, H.S.; Doh, H.M.; Chon, Y.K. Ultimate strength formulation for stiffened plates subjected to combined axial compression, transverse compression, shear force and lateral pressure loadings. *Ships and Offshore Structures*, 2013, Vol.8.
- [15] Zhang, S. A review and study on ultimate strength of steel plates and stiffened panels in axial compression. *Ships and Offshore Structures*, 2016, Vol.11.